2005-07-24

Time-Optimal Nonlinear Feedback Control for the NPSAT1 Spacecraft, IEEE-ASME (2005; Monterey, California)

Sekhavat, Pooya

IEEE

Proceedings of the 2005 IEEE/ASME
International Conference on Advanced Intelligent Mechatronics
Monterey, California, USA, 24-28 July, 2005

Time-Optimal Nonlinear Feedback Control for the NPSAT1 Spacecraft

Pooya Sekhavat [1], **Andrew Fleming** [2] and **I. Michael Ross**[3]

Department of Mechanical and Astronautical Engineering
Naval Postgraduate School
Monterey, CA 93943

Abstract- NPSAT1 is a small satellite being built at the Naval Postgraduate School, and due to launch in January 2006. It uses magnetic actuators and a pitch momentum wheel for attitude control. In this paper, a novel time-optimal sampled-data feedback control algorithm is introduced for closed-loop control of NPSAT1 in the presence of disturbances. The feedback law is not analytically explicit; rather, it is obtained by a rapid re-computation of the open-loop time-optimal control at each update instant. The implementation of the proposed controller is based on a shrinking horizon approach and does not require any advance knowledge of the computation time. Pre-ground-test simulations show that the proposed control scheme performs well in the presence of parameter uncertainties and external disturbance torques.

1 Introduction

In their pioneering work, Bilimoria and Wie [1] showed that eigenaxis maneuvers were, in general, not time-optimal for reorienting a rigid body. In fact, although this is a simple maneuver, it is frequently quite far from optimality. Classical closed-loop control techniques are, in general, ill suited for such time-optimal slew maneuvers. This is due in part to the nonlinear nature of the problem and the inability of classical control techniques to generate time-optimal solutions. Furthermore, the system dynamics is non-Eulerian as a result of the strong coupling between the actuator dynamics and the rigid body. The NPSAT1 spacecraft is one such system initially designed for three-axis magnetic torque control (Fig 1) [2]. Although a pitch bias wheel was subsequently added to the system, this paper addresses the original design without the pitch bias wheel. By solving the optimal control problem, it has been shown that the eigenaxis maneuver for NPSAT1 is also not time-optimal [3]. Inverting actuator dynamics equations to produce actuator inputs leads to singularity problems that continue to plague the ongoing research [4-5].

Fig. 1 NPSAT1 Schematic Image.

Given the absence of a close-form solution to such problems, the traditional approach to nonlinear feedback control must necessarily be abandoned. On the other hand, a conceptually simple approach to controlling such nonlinear systems is by solving the problems online. If such problems can be solved online, there is no need for an off-line design of close-form feedback laws as, by definition, the control system would have acquired this intelligence. In this paper, such an intelligent attitude maneuvering system is designed for the NPSAT1 spacecraft by solving the time-optimal control problem online. Once the initial and final attitudes of the spacecraft are provided, the proposed algorithm computes the nonlinear optimal

[1] Postdoctoral Research Associate
[2] Graduate Student
[3] Professor, Email: imross@nps.edu

control. As a result of parameter uncertainty and external disturbance torques in real applications, the system response deviates from what predicted. Therefore, rather than tracking a pre-computed solution, the control scheme proposed in this paper re-solves the optimal control problem and updates the control command as soon as a new solution is obtained. This results in a sampled-data feedback law which provides optimality in the presence of various types of disturbances [6].

In order to solve the optimal control problem, a spectral algorithm [5-11] programmed into a reusable computer software package DIDO [12] is employed. The basic idea of this spectral algorithm is to, first, seek polynomial approximations for the state, co-state and control functions in terms of their values at the Legendre-Gauss-Lobatto node points [5-11], and, next, solve a sequence of resulting finite-dimensional optimization problems. Such numerical calculation of the time-optimal solution allows for inclusion of all nonlinearities of the system dynamics and the Earth's magnetic field. For further details about the method and its use for real-time optimal control, see references [5-11].

In our previous paper [13], a version of the spectral algorithm was used to solve the slew maneuver problem for NPSAT1 and was shown that the spectral method was capable of providing about 10-30 samples over the minimum-time horizon. In this paper, the analysis is extended by closing the loop of the online computation as well as allowing for disturbance torques, parameter uncertainties and sensor noise to be applied on the system. In essence, this paper presents a comprehensive analysis of a new approach to optimal feedback attitude maneuvering.

2 Problem Formulation

2.1 Kinematic and Dynamic Equations of motion

Let $OXYZ$ and $OX_1Y_1Z_1$ define the orbit frame and the body frame where OZ points from the spacecraft to the earth center, OX follows the negative normal direction to the orbit plane, and OY is defined by the right-hand rule. Using the quaternion representation of the rigid body angular orientation, $\boldsymbol{q} = \begin{pmatrix} q_1 & q_2 & q_3 & q_4 \end{pmatrix}^T$, leads to convenient kinematical expressions involving the Euler symmetric parameters. Thus, the satellite kinematic equations of angular motion with respect to the orbit frame in the body frame are [14]:

$$\dot{\boldsymbol{q}} = \frac{1}{2}\begin{bmatrix} 0 & \omega_z & -\omega_y & \omega_x \\ -\omega_z & 0 & \omega_x & \omega_y \\ \omega_y & -\omega_x & 0 & \omega_z \\ -\omega_x & -\omega_y & -\omega_z & 0 \end{bmatrix}\boldsymbol{q} \tag{1}$$

where ${}^{O}\boldsymbol{\omega}_B^B = \begin{pmatrix} \omega_x, \omega_y, \omega_z \end{pmatrix}^T$ is the rotation rate of the body frame with respect to the orbit frame, expressed in the body frame.

The dynamic equations of angular motion are the Euler's rotational equations of motion [14]:

$$\begin{aligned} \dot{\omega}_1 &= \frac{M_1}{I_1} + \frac{I_2 - I_3}{I_1}\omega_2\omega_3 \\ \dot{\omega}_2 &= \frac{M_2}{I_2} + \frac{I_3 - I_1}{I_2}\omega_3\omega_1 \\ \dot{\omega}_3 &= \frac{M_3}{I_3} + \frac{I_1 - I_2}{I_3}\omega_1\omega_2 \end{aligned} \tag{2}$$

where ${}^{N}\boldsymbol{\omega}_B^B = \begin{pmatrix} \omega_1, \omega_2, \omega_3 \end{pmatrix}^T$ is the rotation rate of the body frame with respect to the inertial frame (expressed in the body frame), I_i (i=1..3) are the principal moments of inertia, and M_i (i=1..3) are the external torque acting on the spacecraft about the principal axes. The direction cosine matrix, C, is a coordinate transformation that maps the angular velocity from ${}^{O}\boldsymbol{\omega}_B^B$ to ${}^{N}\boldsymbol{\omega}_B^B$ as follows [14]:

$${}^{N}\boldsymbol{\omega}_B^B = {}^{O}\boldsymbol{\omega}_B^B + {}^{B}C^{O}\,{}^{N}\boldsymbol{\omega}_O^O \tag{3}$$

$${}^{B}C^{O} = \begin{bmatrix} q_1^2 - q_2^2 - q_3^2 + q_4^2 & 2(q_1q_2 + q_3q_4) & 2(q_1q_3 - q_2q_4) \\ 2(q_1q_2 - q_3q_4) & q_2^2 - q_1^2 - q_3^2 + q_4^2 & 2(q_2q_3 + q_1q_4) \\ 2(q_1q_3 + q_2q_4) & 2(q_2q_3 - q_1q_4) & q_3^2 - q_1^2 - q_2^2 + q_4^2 \end{bmatrix} \tag{4}$$

Therefore, when ${}^{N}\boldsymbol{\omega}_O^O = \begin{pmatrix} 0 & -\omega_0 & 0 \end{pmatrix}^T$ is the angular velocity of the orbit with respect to the inertial frame (expressed in the orbit frame), $\omega_x, \omega_y,$ and ω_z in (1) can be replaced according to the following equation:

$$\begin{bmatrix} \omega_1 \\ \omega_2 \\ \omega_3 \end{bmatrix} = \begin{bmatrix} \omega_x \\ \omega_y \\ \omega_z \end{bmatrix} - \omega_0 \begin{bmatrix} 2(q_1q_2 + q_3q_4) \\ q_2^2 - q_1^2 - q_3^2 + q_4^2 \\ 2(q_2q_3 - q_1q_4) \end{bmatrix} \tag{5}$$

The spacecraft states can be now summarized by $\boldsymbol{x}_{7\times 1} = \begin{pmatrix} \boldsymbol{q} & \boldsymbol{\omega} \end{pmatrix}^T$ where $\boldsymbol{\omega} = {}^{N}\boldsymbol{\omega}_B^B$.

2.2 Actuation Torques

The actuation toques are generated as a result of interaction between the Earth's magnetic field and the

spacecraft's magnetic torque rods:

$$\boldsymbol{M} = {}^{N}\boldsymbol{m}^{\boldsymbol{B}} \times {}^{N}\boldsymbol{B}^{\boldsymbol{B}} \tag{6}$$

where ${}^{N}\boldsymbol{m}^{\boldsymbol{B}} = \begin{pmatrix} m_1 & m_2 & m_3 \end{pmatrix}^T$ is the magnetic dipole moment of the torque rods and ${}^{N}\boldsymbol{B}^{\boldsymbol{B}} = \begin{pmatrix} B_x & B_y & B_z \end{pmatrix}^T$ is the Earth's magnetic field both with respect to the inertial frame and expressed in the body frame. Therefore, in the absence of disturbance torques, the net external toques applied on the spacecraft are:

$$\begin{aligned} M_1 &= m_2 B_z - m_3 B_y \\ M_2 &= -m_1 B_z + m_3 B_x \\ M_3 &= m_1 B_y - m_2 B_x \end{aligned} \tag{7}$$

2.3 The Earth's Magnetic Field

The Earth's magnetic field approximated by a dipole model and represented in the orbit frame, ${}^{N}\boldsymbol{B}^{\boldsymbol{O}}$, can be represented as follows [15]:

$${}^{N}\begin{bmatrix} B_{x_O} \\ B_{y_O} \\ B_{z_O} \end{bmatrix}^{O} = \frac{M_e}{r_0^3}\begin{bmatrix} C\alpha(SiC\varepsilon - S\varepsilon CiCu) - S\alpha SuS\varepsilon \\ -CiC\varepsilon - S\varepsilon CiCu \\ 2C\alpha SuS\varepsilon + 2S\alpha(SiC\varepsilon - S\varepsilon CiCu) \end{bmatrix} \tag{8}$$

where *C*=*Cos*, *S*=*Sin*, M_e is the magnetic dipole moment of the Earth (7.953x10^{15} Wb.m), *i* is the orbit inclination, ε is the magnetic dipole tilt, and r_0 is the distance from center of spacecraft to the center of the earth. The variables $\alpha = \omega_0 t$ and $u = \omega_e t$ are calculated using the orbital angular velocity (ω_0), the spin rate of the Earth (ω_e), and the time *t* which is zero when the satellite is at the ascending node of the satellite orbit. Before substituting (8) into (7), $\boldsymbol{B}$ should be transformed from the orbit frame to body frame:

$${}^{N}\boldsymbol{B}^{\boldsymbol{B}} = {}^{B}C^{O}\,{}^{N}\boldsymbol{B}^{\boldsymbol{O}} \tag{9}$$

where ${}^{B}C^{O}$ is as defined in (4).

Substitution of equation (5) into (1) and combination of equations (2), (7), (8) and (9) lead to the complete nonlinear kinematic and dynamic equations of motion.

2.4 Time-Optimal Rest-to-Rest Reorientation

The problem addressed in this study is to find the optimal control vector ${}^{N}\boldsymbol{m}^{\boldsymbol{B}} = \begin{pmatrix} m_1 & m_2 & m_3 \end{pmatrix}^T$ that minimizes the maneuver time for a spacecraft undergoing a rest-to-rest reorientation using magnetic actuators. Therefore, the cost function is

$$J = \int_{t_0}^{t_f} dt = t_f - t_0 \tag{10}$$

subject to the control constraint (torque rod limitations),

$$|m_i| \le 30A \cdot m^2 \quad (i=1..3) \tag{11}$$

the initial conditions,

$$\begin{aligned} &\omega_x(t_0) = 0, \quad \omega_y(t_0) = 0, \quad \omega_z(t_0) = 0 \\ &q_1(t_0) = q_2(t_0) = q_3(t_0) = 0, \quad q_4(t_0) = 1 \end{aligned} \tag{12}$$

and the terminal conditions,

$$\begin{aligned} &\omega_x(t_f) = \omega_y(t_f) = \omega_z(t_f) = 0 \\ &q_1(t_f) = \sin(\phi/2),\ q_2(t_f) = q_3(t_f) = 0,\ q_4(t_f) = \cos(\phi/2) \end{aligned} \tag{13}$$

The angle ϕ is the principal rotation angle about the *x* axis [3].

The first step in solving the optimal control problem is to form the Hamiltonian:

$$H(\boldsymbol{\lambda}, \boldsymbol{x}, \boldsymbol{m}, t) = F(\boldsymbol{x}, \boldsymbol{m}, t) + \boldsymbol{\lambda}^T \boldsymbol{f}(\boldsymbol{x}, \boldsymbol{m}, t) \tag{14}$$

where *F* is the Lagrange cost and $\boldsymbol{f}$ is the vector field of the right-hand-side of the differential equations of motion. Thus,

$$\begin{aligned} H = {} & \frac{\lambda_{q_1}}{2}(\omega_1 q_4 - \omega_2 q_3 + \omega_3 q_2 + \omega_0 q_3) + \frac{\lambda_{q_2}}{2}(\omega_1 q_3 + \omega_2 q_4 - \omega_3 q_1 + \omega_0 q_4) \\ & + \frac{\lambda_{q_3}}{2}(-\omega_1 q_2 + \omega_2 q_1 + \omega_3 q_4 - \omega_0 q_1) + \frac{\lambda_{q_4}}{2}(-\omega_1 q_1 - \omega_2 q_2 - \omega_3 q_3 - \omega_0 q_2) \\ & + \lambda_{\omega_1}\left\{\frac{1}{I_1}(m_2 B_z - m_3 B_y) + \frac{I_2 - I_3}{I_1}\omega_2\omega_3\right\} \\ & + \lambda_{\omega_2}\left\{\frac{1}{I_2}(m_3 B_x - m_1 B_z) + \frac{I_3 - I_1}{I_2}\omega_1\omega_3\right\} \\ & + \lambda_{\omega_3}\left\{\frac{1}{I_3}(m_1 B_y - m_2 B_x) + \frac{I_1 - I_2}{I_3}\omega_1\omega_2\right\} \end{aligned} \tag{15}$$

According to Pontryagin's Minimum Principle, the optimal control must minimize the Hamiltonian with respect to control. Since the Hamiltonian of the problem under study is subject to an inequality constraint on the control variable, we apply the Karush-Kuhn-Tucker Theorem and form the Lagrangian of the Hamiltonian,

$$\bar{H} = H + \boldsymbol{\mu}^T \boldsymbol{h} \tag{16}$$

where μ_i (i=1..3) is a KKT multiplier and $\boldsymbol{h}$ is the control constraint vector [see (11)]. Therefore, the KKT theorem gives the following necessary condition for the optimal trajectory:

$$\frac{\partial \bar{H}}{\partial m_i} = \frac{\partial H}{\partial m_i} + \left(\frac{\partial \boldsymbol{h}}{\partial m_i}\right)^T \boldsymbol{\mu} = 0 \qquad (17)$$

By substituting (11) and (15) into (17), the necessary conditions for the Hamiltonian minimization are

$$\begin{aligned}
&\frac{\lambda_{\omega_3}}{I_3} B_y - \frac{\lambda_{\omega_2}}{I_2} B_z + \mu_1 = 0 \\
&\frac{\lambda_{\omega_1}}{I_1} B_z - \frac{\lambda_{\omega_3}}{I_3} B_x + \mu_2 = 0 \\
&\underbrace{\frac{\lambda_{\omega_2}}{I_2} B_x - \frac{\lambda_{\omega_1}}{I_1} B_y}_{S_i} + \underbrace{\mu_3}_{mu_i} = 0
\end{aligned} \qquad (18)$$

and the multiplier-constraint pair must satisfy the complementarity conditions of the KKT Theorem:

$$\mu_i \begin{cases} \leq 0 & \\ = 0 & \text{if} \\ \geq 0 & \\ \text{unrestricted} & \end{cases} \begin{cases} h_i(\boldsymbol{m},t) = h_i^L(\boldsymbol{m},t) \\ h_i^L(\boldsymbol{m},t) < h_i(\boldsymbol{m},t) < h_i^U(\boldsymbol{m},t) \\ h_i(\boldsymbol{m},t) = h_i^U(\boldsymbol{m},t) \\ h_i^L(\boldsymbol{m},t) = h_i^U(\boldsymbol{m},t) \end{cases} \qquad (19)$$

Although the time-dependence of the Earth magnetic filed results in a time-varying Hamiltonian, the end-point Lagrangian [3]

$$\bar{E}(\boldsymbol{\upsilon}, \boldsymbol{x}_f, t_f) = E(\boldsymbol{x}_f, t_f) + \boldsymbol{\upsilon}^T \boldsymbol{e}(\boldsymbol{x}_f, t_f) \qquad (20)$$

can be used in the Hamiltonian Value Condition to determine the final value of the Hamiltonian:

$$H[t_f] + \frac{\partial \bar{E}}{\partial t_f} = 0 \qquad (21)$$

For the slew maneuver under study, the end manifold $\boldsymbol{e}(\boldsymbol{x}_f, t_f)$ is

$$\begin{aligned}
\boldsymbol{e}(\boldsymbol{x}_f, t_f) = \Big[& q_1^f - \sin(\phi/2) \quad q_2^f \quad q_3^f \quad q_4^f - \cos(\phi/2) \\
& \omega_1^f \quad \omega_2^f + \omega_0 \cos(\phi) \quad \omega_3^f - \omega_0 \sin(\phi) \Big]^T = \mathbf{0}
\end{aligned} \qquad (22)$$

Therefore, (10), (21) and (22) lead to the following condition on the Hamiltonian final value:

$$H[t_f] + 1 = 0 \Rightarrow H[t_f] = -1 \qquad (23)$$

Throughout this study, the above analysis is used for validation of the calculated solutions. The Legendre Pseudospectral Method (through its Covector Mapping Theorem) provides costate information at the nodes that are required to evaluate necessary conditions (18) and (23) for optimality.

3 Sampled-Data Feedback Control

The basic idea of the sampled-data closed-loop spacecraft control is shown in Fig 2. Knowing the initial conditions (t_0, $\boldsymbol{x}_0$), and the desired final states, $\boldsymbol{x}_f$, an off-line run of the open-loop time-optimal control using the optimal control software DIDO [12] provides the initial control signal, m_0^* and an estimate of the final time, t^f. These are then used as the start-up values for closed-loop control. During the on-line closed-loop control, a new open-loop optimal solution is re-generated using the optimal control software DIDO [12] and fed back in a form of sampled–data feedback control law. When each new open-loop solution (and therefore its calculation time) is available, the current states of the spacecraft under the previous open-loop control are determined based on the actual computation time of the new solution. The re-optimized optimal control signal is then applied to the evolved status of the space-craft.

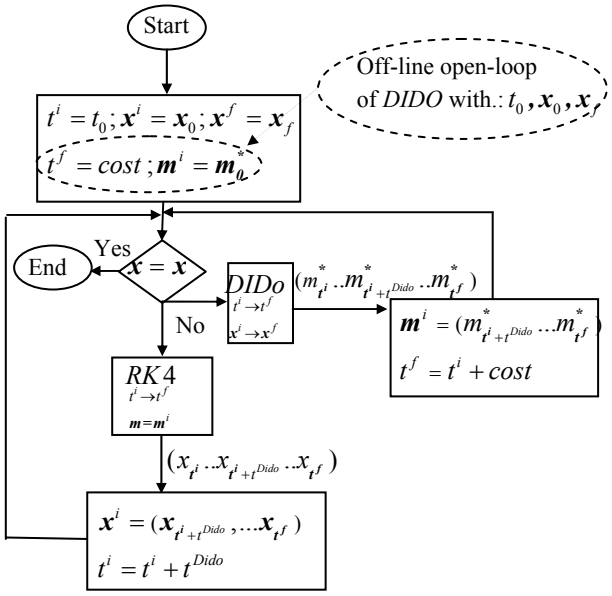

Fig. 2 Closed-loop Control Algorithm.

4 Results and Discussions

The rest-to-rest roll (x-axis slew) maneuver of NPSAT1 is studied to illustrate the performance of the above on-line closed-loop control scheme. For the 135° maneuver ($\phi = 135^\circ$), the final desired end points are [see (13)]:

$$\boldsymbol{q}^T(t_f) = \begin{bmatrix} 0.924 & 0 & 0 & 0.383 \end{bmatrix}^T$$

$$\left({}^{O}\boldsymbol{\omega}_{B}^{B}\right)^{T}(t_f)=\begin{bmatrix}0 & 0 & 0\end{bmatrix}^{T} \quad (24)$$

The parameters of NPSAT1 mission are listed in Table 1.

Table 1 Data for NPSAT1

Altitude	~ 560 km
Inclination	~ 35.4 deg
I_1	~ 5 kg.m^2
I_2	~ 5.1 kg.m^2
I_3	~ 2 kg.m^2
$I_{12}= I_{13}= I_{23}$	~ 0 kg.m^2
Max. Dipole Moment	~ 30 Amp.m^2

4.1 Open-loop Control Solution

For the 135 degree x-axis slew maneuver, the open-loop time-optimal solution of the system is shown in Fig 3. It is seen that the time-optimal bang-bang control structure can bring the satellite to the final desired attitude within 220 seconds. Both the variation in the quaternions q_1 & q_2 and the non-zero angular rates ω_1 & ω_2 indicate that the maneuver is not an eigenaxis slew. The current tolerances of 1 degree on the final angle and 0.06 deg/s on angular rates are shown in dash-dotted lines.

To ensure the feasibility of the open-loop solution, the solution is propagated via separate ODE Runge-Kutta propagator. Results showed that the system response does meet the end point conditions. As a measure of verifying the optimality of the open-loop solution, the Hamiltonian Minimization Conditions (18) were examined using the values of the switching functions (the partial derivative of the Hamiltonian with respect to the control vector) and KKT multipliers derived from the optimization software. The sum of the switching function S_i and the KKT multiplier μ_i [see (18)] should be equal to zero if the Hamiltonian is minimal. This condition also verified optimality of the open-loop solution. Finally, according to (23), the numerical final value of the Hamiltonian should be equal to -1 if the solution is optimal. Figure 5 shows the system's Hamiltonian evolution throughout the maneuver. Due to the time-dependence of the Earth magnetic field, the system Hamiltonian is not constant. However, the final value of the Hamiltonian at the end manifold (-1.0642) matches the theoretically calculated value (-1) with % 93.6 accuracy.

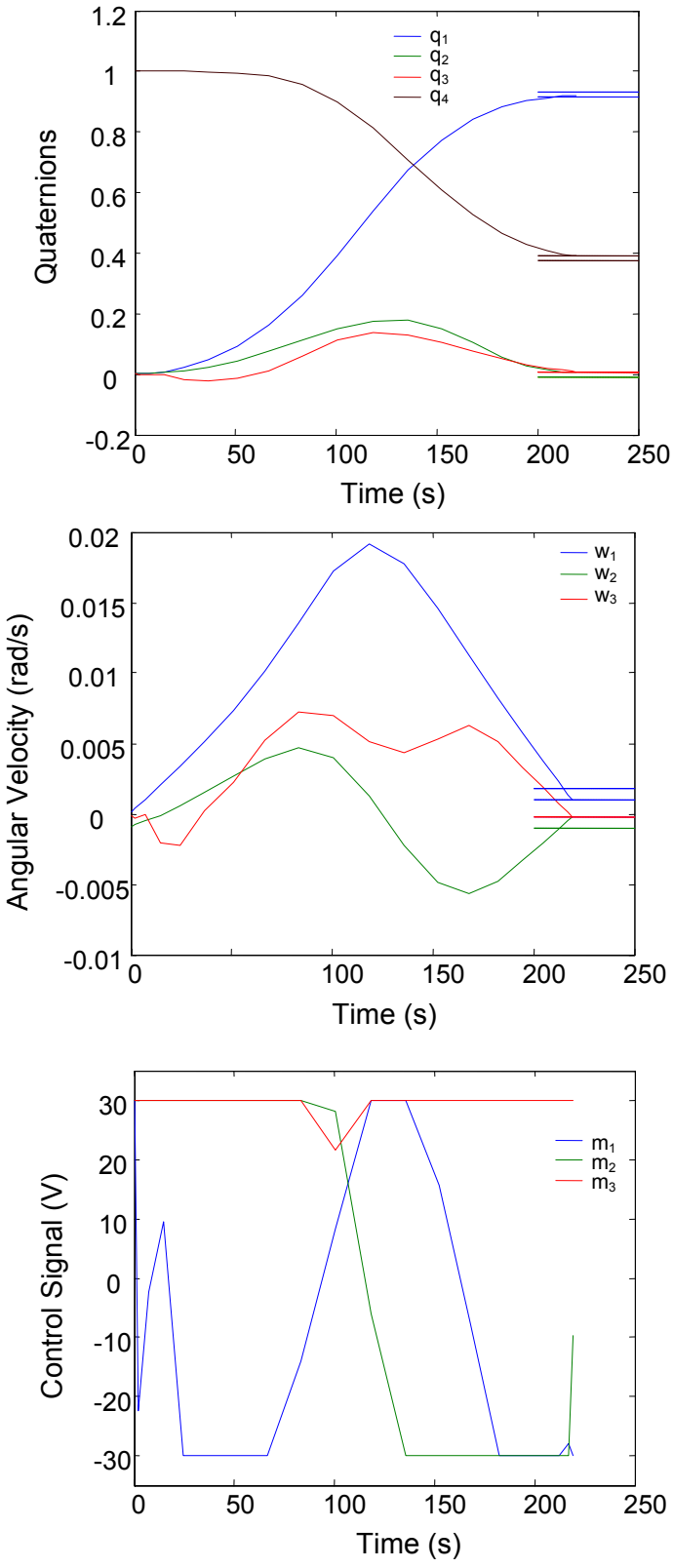

Fig 3 Open-loop optimal control.

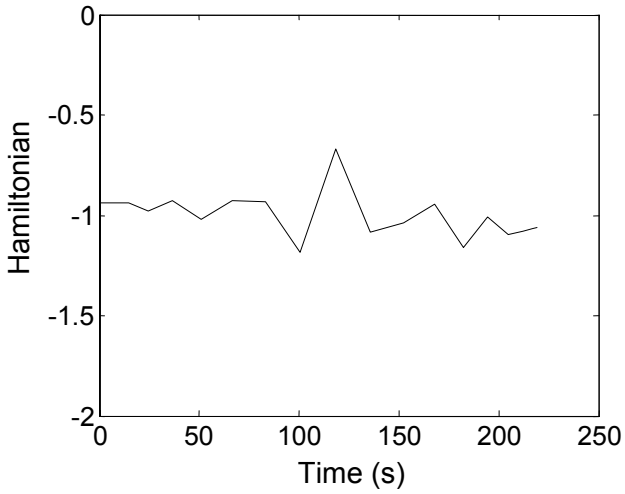

Fig. 4 Hamiltonian of the open-loop system.

4.2 Closed-loop Control

The open-loop time-optimal solution derived in Section 4.1 does not take any exogenous disturbance into account. Disturbance in real applications is inevitably introduced due to parameter uncertainties, sensor measurement errors, or unknown external toques and can considerably degrade the performance of the system. This is shown in Fig 5 by applying the open-loop time-optimal control signals obtained in Section 4.1 (Fig 3) on a real system with disturbance. As parameter uncertainty, moments of inertia are deviated for 5% and three external disturbance torques are included for a period of 130 *s* between *t*=50 and *t*=180 seconds of motion.

$$M_{d_1} = 10.0\text{x}10^{-5} \quad N.m$$
$$M_{d_2} = 10.0\text{x}10^{-5} \quad N.m \qquad (25)$$
$$M_{d_3} = 10.0\text{x}10^{-5} \quad N.m$$

Note that during the numerical propagations, the numerical errors in propagation can play the role of the errors in sensor measurements.

The system response under the above disturbances is shown in Fig 5 (thick lines). It can be clearly seen that application of the open-loop time optimal solution to maneuver a real system fails.

Next the closed-loop control procedure introduced in Section 3 is applied. According to Bellman's Principle of Optimality, given an optimal open-loop trajectory, the re-optimized closed-loop trajectories should follow the original open-loop response. However, that is valid for a system without disturbance. In the presence of disturbance, the time-optimal trajectory changes

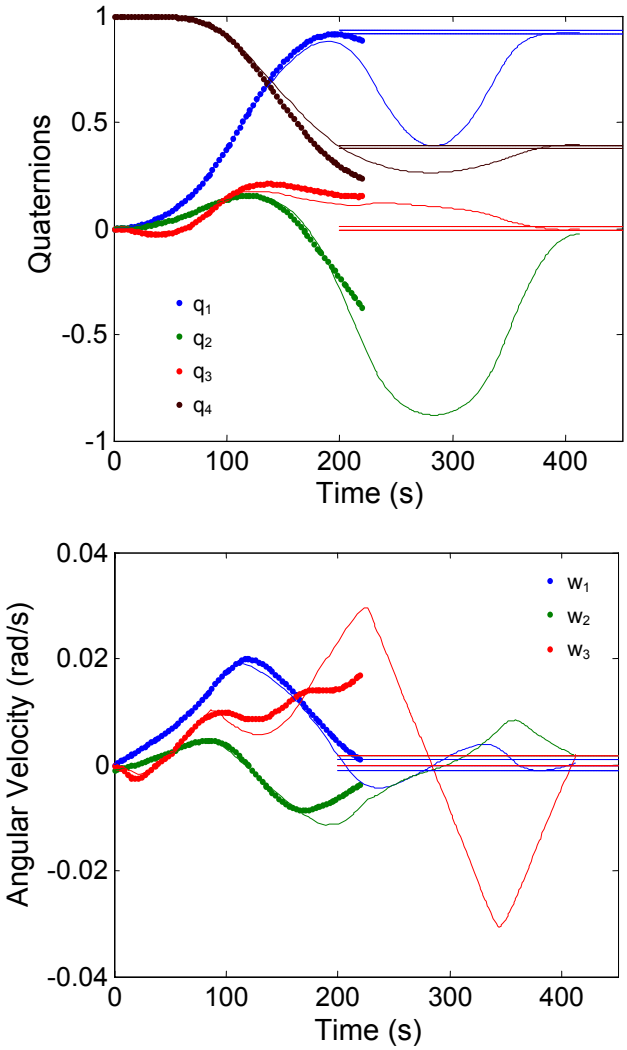

Fig 5 System response with disturbance. ….Open-loop, —— Closed-loop.

repeatedly and a new optimal trajectory is feedback to the system as each feedback instant. This results in a different control trajectory as shown in Fig 7. The behavior of the disturbed system under such a uniquely computed control trajectory is presented by thin solid lines in Fig 5. The figure shows that the proposed closed-loop control scheme is capable of counteracting the disturbances and achieving the desired attitude. It also shows that the time optimal maneuver in the presence of various disturbances takes longer to complete. Note that application of the control scheme introduced in this paper does not require the prior knowledge of the re-optimizing computation times for feedback sampling. Therefore, the actual re-optimizing computation times are used to propagate the actual states at the end of each

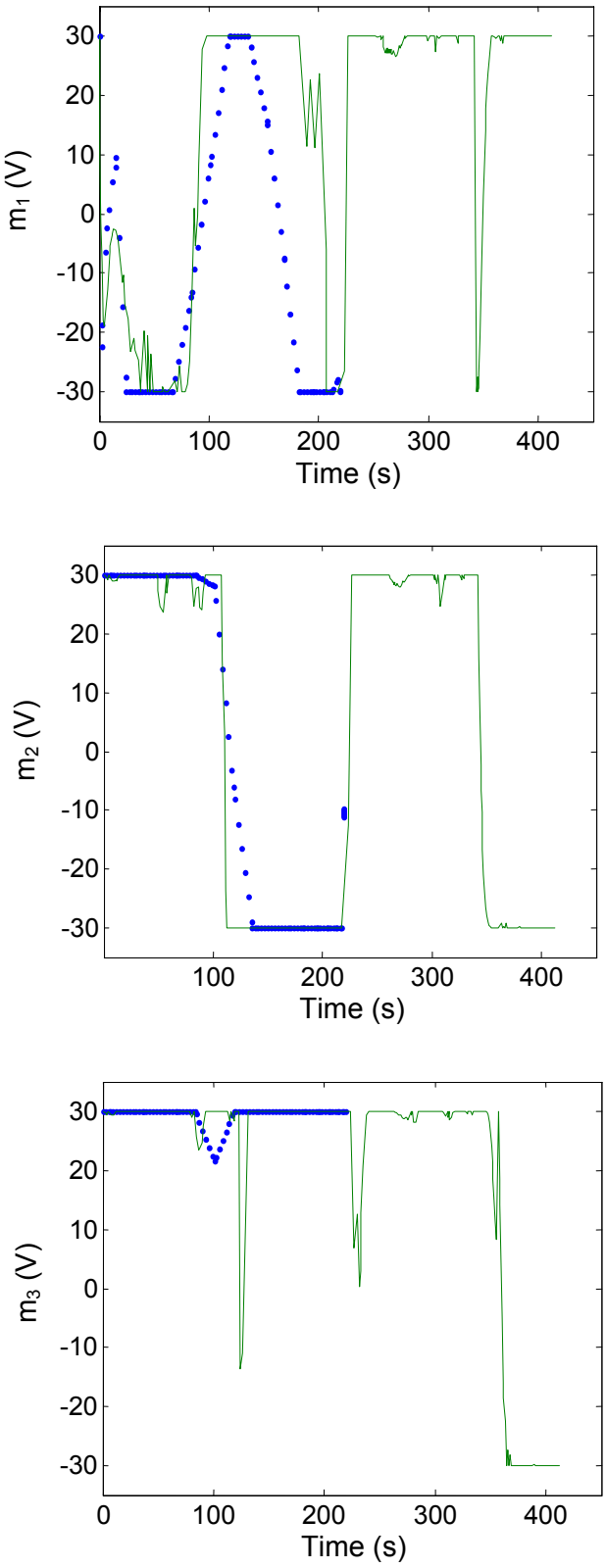

Fig. 6 Control trajectory.
---- Open-loop, —— Closed-loop.

re-optimization. These are, in fact, the actual time spent for each re-optimizing calculation by DIDO. For the system under study, computation of the first off-line open-loop time-optimal control trajectory takes 10 seconds and the subsequent open-loop optimal control updates are computed within 0.84 to 10.5 seconds. The complete spectrum of feedback computation times for the overall maneuver is illustrated in Fig. 7.

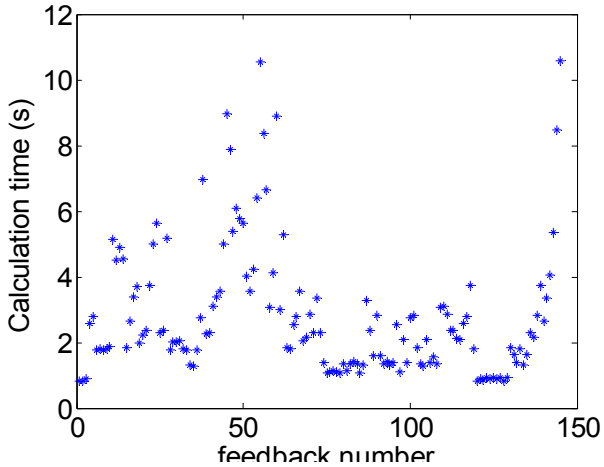

Fig. 7 Feedback computation times for the system with disturbance.

5 Conclusions

Successive time-optimal open-loop solutions for the slew maneuver of a magnetically actuated spacecraft were used to construct a sampled–data feedback control law. In lieu of the improvements of computational power and numerical methods, it was shown that rapid re-computation of the open-loop time-optimal control can effectively be used for on-line time optimal slew maneuvers of spacecrafts in the presence of various disturbances and uncertainties. One important feature of the control scheme is it does not require any advance knowledge of feedback computation times. The well performance of the proposed scheme in reducing the final steady-state errors is shown via pre-ground-test simulations.

References

[1] Bilimoria, K. D., and Wie, B., "Time-Optimal Three-Axis Reorientation of a Rigid Spacecraft," *Journal of Guidance, Control, and Dynamics,* Vol.16, No.3, 1993, pp. 446-452.

[2] Leonard, B. S., "NPSAT1 Magnetic Attitude Control System," SSC02-V-7.

[3] Fleming, A. "Real-time Optimal Slew Maneuver Design and Control." Astronautical Engineer's Thesis, US Naval Postgraduate School, 2004.

[4] Wie, B., Bailey, D., and Heiberg, C. "Rapid Multitarget Acquisition and Pointing Control of Agile Spacecraft", *Journal of Guidance, Control, and Dynamics,* Vol. 25, No.1, 2002, pp. ?.

[5] Ford, K. A., and Hall, C. D., "Singular Direction Avoidance Steering for Control Moment Gyros", *Journal of Guidance, Control, and Dynamics,* Vol. 23, No.4, 2000, pp. ?.

[6] Bryson, A. E., and Ho, Y., *Applied Optimal Control*, Taylor & Francis Publishing, NY, 1975.

[7] Ross, I. M. and Fahroo, F., "Legendre Pseudospectral Approximations of Optimal Control Problems," *Lecture Notes in Control and Information Sciences,* Vol. 295, Springer-Verlag, New York, 2003, pp 327-342.

[8] Ross, I. M. and Fahroo, F., "Issues in the Real-Time Computation of Optimal Control," *Mathematical and Computer Modelling*, An International Journal, Vol. 40, Pergamon Publication, to appear.

[9] Ross, I. M. and Fahroo, F., "Pseudospectral Knotting Methods for Solving Optimal Control Problems," *Journal of Guidance, Control and Dynamics*, Vol. 27, No. 3, pp.397-405, 2004.

[10] Ross, I. M., Fahroo, F., and Gong, Q., "A Spectral Algorithm for Pseudospectral Methods in Optimal Control," *Proc. 10th Int. Conf. Cybernetics and Information Technologies, Systems and Applications,* 2004, Orlando, FL.

[11] Gong, Q., Ross, I. M., Kang, W. and Fahroo, F., "Convergence of Pseudospectral Methods for Constrained Nonlinear Optimal Control Problems," *Proc 6th IASTED Int. Conf. Intelligent Systems and Control*, 2004, Honolulu, HI.

[12] Ross, I. M., and Fahroo, F., "User's Manual for DIDO 2002: A MATLAB Application Package for Dynamic Optimization," NPS Technical Report AA-02-002, Department of Aeronautics and Astronautics, Naval Postgraduate School, Monterey, CA, June 2002.

[13] Yan, H., Fleming, A., Ross, I. M. and Alfriend, K. T., "Real-Time Computation of Time-Optimal Magnetic Attitude Control," *15th AAS/AIAA Space Flight Mechanics Conference*, Copper Mountain, CO, 2005. Paper AAS 05-233.

[14] Wertz, J. R. (ed.), *Spacecraft Attitude Determination and Control*, D. Reidel, Boston, 1978, pp. 779-786.

[15] Wheeler, P.C., "Magnetic Attitude Control of Rigid, Axially Symmetric Spinning Satellites in Circular Earth Orbits", NASA Paper CR-313, 1971.